# Structures and electronic properties of $B_2Si_6^{-/0/+}$: anion photoelectron spectroscopy and theoretical calculations

Guo-Jin Cao,[*a] Sheng-Jie Lu,[bc] Hong-Guang Xu,[bc] Xi-Ling Xu[*bc] and Wei-Jun Zheng[bc]

We measured the photoelectron spectrum of $B_2Si_6^-$ anion and investigated the structures and electronic properties of $B_2Si_6^-$ anion as well as those of its neutral and cationic counterparts with quantum chemical calculations. The vertical detachment energy (VDE) of the $B_2Si_6^-$ anion has been measured to be $2.40 \pm 0.08$ eV. Through global minimum searches and CCSD(T) calculations, we have identified that the lowest-energy structures of $B_2Si_6^q$ ($q = -1, 0, +1$) are peculiar structures with a Si atom hanging over a distorted bowl-like $B_2Si_5$ framework. Quasi-planar or planar isomers have also been identified for the $B_2Si_6$ cluster at $-1$, 0, and $+1$ charge states. The quasi-planar and planar isomers are higher in energy than their bowl-like counterparts by at least 0.20 eV. The symmetries of the quasi-planar isomers varied at different charge states, ranging from $C_s$ to $C_{2h}$, then to $D_{2h}$ respectively for the $-1$, 0, and $+1$ charge states. The reducing of the symmetry from $+1$ charge state to $-1$ charge state is more likely due to the Jahn–Teller effect upon the addition of electrons.

## 1. Introduction

Silicon-based compounds have attracted tremendous attention because of their importance in the semiconductor industry.[1–4] They have aromaticity, size-dependent structural characteristics, as well as distinctive physiochemical properties.[5] In particular, they have been used as one of the most important p-type dopants in crystalline silicon.[6,7] Boron-silicon compounds have high melting points and high hardness. Their conductivity increases with the increasing concentration of boron.[5,8,9] Compared with carbon, silicon is more reluctant to form unsaturated compounds.[10–14] Although the synthesis and isolation of stable unsaturated silicon compounds are a great challenge, some silicon–silicon multiple-bonded compounds were identified in the last decades. In 1981, a Si═Si double-bonded compound, silaethene, was isolated by Brook et al.[15] In the same year, West et al.[10] synthesized and isolated a stable compound containing a Si═Si double bond, tetramesityldisilene. Since then, many other interesting stable unsaturated silicon compounds have been investigated extensively.[16–24]

Scientists have made great efforts to search for compounds with planar aromatic six-membered silicon rings (c-Si₆) over the past decades because they may be used as highly stable two-dimensional (2D) aromatic nanomaterial. The cyclo-trisilenylium ion[25] and cyclobutadiene dianion[26] have been found to be the potentially aromatic compounds based on the planar three-membered or four-membered silicon rings. As the silicon analogues of benzene, compounds with planar aromatic c-Si₆ have been of great interest in the silicene field.[27,28] The planar $D_{6h}$ c-Si₆ unit in Si₆H₆ is less stable than the chair-like $D_{3d}$ structure due to the pseudo-Jahn–Teller effect.[29,30] The dark green crystals of an isomer of Si₆H₆ with the proposed dismutational aromaticity[31] were synthesized by Abersfelder et al.[22] It has a chair-like conformation in line with the theoretical results.[29,30] Subsequently, a cage isomer of hexasilabenzene was investigated experimentally by Abersfelder et al.[32,33] and Kratzert et al.[34] In addition, several planar $D_{6h}$ c-Si₆ structures have been suggested by theoreticians. These planar benzene-like structures can be formed by substituting Si atoms by C atoms in silabenzenes.[35] It has also been proposed that anionic systems c-Si₆²⁻, c-Si₆⁴⁻, and c-Si₆⁶⁻ could be planar.[36–38] Zdetsis et al.[27] have predicted that Si₆Li₆ with $D_{2h}$ symmetry could be formed by the reduction of the c-Si₆⁶⁻ anion in the presence of lithium. Recently, the c-BSi₃ silicene containing planar aromatic $D_{6h}$ c-Si₆ rings has been predicted by theory to be the global minimum of the BSi₃ monolayer and possesses metallic character.[39]

There have been many experimental and theoretical investigations on the structural and electronic properties of small size Si$_n$B$_m$ clusters.[8,9,39–50] Cline et al.[8,9] have reported the existence of two new silicon borides SiB₄ and SiB₆ in silicon-boron

[a]Institute of Molecular Science, Shanxi University, Taiyuan 030006, China. E-mail: caoguojin@sxu.edu.cn

[b]Beijing National Laboratory for Molecular Sciences, State Key Laboratory of Molecular Reaction Dynamics, Institute of Chemistry, Chinese Academy of Sciences, Beijing 100190, China. E-mail: xlxu@iccas.ac.cn

[c]University of Chinese Academy of Sciences, Beijing 100049, P. R. China

systems. Bernardo and Morrison[40] performed a theoretical study on the structures and binding energies of $SiB_n^+$ ($n = 1$–4) and suggested that $SiB_n^+$ ($n = 1$–4) cluster cations prefer planar boron networks with silicon located at the edge site. The high- and low-spin states of BSi were calculated by Boldyrev and Simons[41] and were confirmed by Knight et al.[42] using electron spin resonance (ESR) spectroscopy technology. Verhaegen et al.[43] and Viswanathan et al.[44] have studied the thermochemistry of BSi, $BSi_2$, and $BSi_3$. Yamauchi et al.[45] have investigated the geometric and electronic properties of $B_{12}$ in silicon crystalline and found that the lowest-lying isomer of $B_{12}$ in silicon crystalline is icosahedral. The low-lying excited electronic states and structures of $BSi_2$, $B_2Si$, and $B_2Si_2$ were investigated by Davy et al. using the B3LYP method.[46] Sun et al.[47] have investigated $BSi_m^-$ ($m = 1$–6) cluster anions using time-of-flight mass spectrometry and quantum chemical calculations. Tam et al.[50] studied the structures, thermochemical properties and growth mechanism of $Si_nB^q$ ($n = 1$–10; $q = -1$, 0, +1) and found that $Si_9B$ and $Si_{10}B$ exhibit endohedral structures. Dai et al.[51] conducted a first-principle theoretical study on the structures of 2D boron-silicon compounds, and found that $B_nSi$ ($n = 1$–3, 5, 6) and $BSi_m$ ($m = 3$, 4) clusters prefer planar $sp^2$-Si structures. Recently, Dopfer and co-workers reported a combined infrared-ultraviolet two-color ionization (IR-UV2CI) spectroscopy and quantum chemical study on $BSi_6$, and found that the most stable structure of $BSi_6$ is a distorted pentagonal bipyramid.[52]

In order to get insight into the structural and electronic properties of boron-doped silicon clusters, in this work we carried out a combined photoelectron spectroscopy and quantum chemical study on $B_2Si_6^{-/0/+}$.

## 2. Experimental and theoretical methods

### 2.1 Experimental method

The experiments were carried out on a home-built apparatus consisting of a time-of-flight mass spectrometer and a magnetic-bottle photoelectron spectrometer, which has been described elsewhere.[53] The $B_2Si_6^-$ anion was produced by laser vaporization of rotating and translating disk targets (13 mm diameter; B/Si molar ratio of 1 : 2) with the second harmonic (532 nm) of a nanosecond Nd:YAG laser (Continuum Surelite II-10). Helium gas with a backing pressure of 5.0 atm. was delivered through a pulsed valve into the laser ablation source to cool the formed $B_2Si_6^-$ anion. The $B_2Si_6^-$ anion was mass-selected and then photodetached with the fourth harmonic light beam from another Nd:YAG laser (Continuum Surelite II-10, 266 nm). The resultant electrons were energy-analyzed by the magnetic-bottle photoelectron spectrometer. The photoelectron spectrum was calibrated using the spectrum of $Cu^-$ anion taken at the similar conditions. The resolution of the photoelectron spectrometer was approximately 40 meV for electrons with 1 eV kinetic energy.

### 2.2 Theoretical method

The theoretical calculations of $B_2Si_6^q$ ($q = -1$, 0, +1) were performed using the Becke 3-parameter-Lee–Yang–Parr (B3LYP) density functional method as implemented in the GAUSSIAN 09 program package.[54] Global minimum searches were carried out using the basin-hopping (BH) method[55] at the DFT level. Low-lying structures were fully optimized using the B3LYP method with the aug-cc-pVTZ basis set. We tested the theoretical method by calculating the bond length of B–Si (1.917 Å, $^4\Sigma^-$), which is in good agreement with the bond length calculated with the MP2 method in the literature (1.905 Å).[42] The vibrational frequencies were calculated to confirm whether their structures are real local minima. The zero-point energies (ZPEs) corrections were included for all calculated energies. For more reliable energies, the CCSD(T) single-point calculations were performed using the Molpro2012 program[56] at the B3LYP/aug-cc-pVTZ geometries. The first VDE was calculated based on the energy difference between the neutral and anion at the ground state geometry of the anion. The excited-state energies of the neutrals were calculated by using the time-dependent density functional theory (TD-DFT) method.[57] The statistical average of orbital potentials (SAOP) functional was employed and all-electron basis sets TZ2P were used for B and Si. Simultaneously, the higher VDE values were also approximated using the generalized Koopman's theorem[58] at the DFT/CAMY-B3LYP[59] level. The TD-DFT and DFT/CAMY-B3LYP[59] calculations were carried out on these clusters using Amsterdam Density Functional program (ADF 2013.01).[60–62]

The natural bond orbital (NBO 5.0)[63,64] analyses of $B_2Si_6^q$ ($q = -1$, 0, +1) were also performed to gain insights into the natural electron configurations of the valence orbitals and natural charges of these clusters. To further understand the nature of B–Si bonds in these boron-silicon complexes, we analyzed the density of state and adaptive natural density partitioning (AdNDP[65]) using the Multiwfn 2.6.1 package.[66]

## 3. Experimental results

The photoelectron spectrum of $B_2Si_6^-$ anion obtained with 266 nm photons is shown in Fig. 1. The spectral features are labeled with letters (X, A, B, and C), which correspond to the transitions from the ground state of $B_2Si_6^-$ anion to the ground and excited states of $B_2Si_6$ neutral. The adiabatic detachment energy (ADE) and vertical detachment energies (VDEs) estimated from the photoelectron spectrum are summarized in Table 1. The spectrum of $B_2Si_6^-$ anion is characterized by a small peak centered at 2.40 eV, a small shoulder centered at 3.61 eV, a broad feature centered at 3.90 eV, followed by a sharp peak centered at 4.27 eV. Because the instrumental resolution shows a significant influence on the broadening of the photoelectron spectrum, the ADE was determined by adding the instrumental resolution to the onset of the first peak in the spectrum. The onset of the first peak was determined by drawing a straight line along the leading edge of that peak across the baseline of the spectrum. The ADE of $B_2Si_6^-$ anion estimated from the experimental spectrum is 2.15 eV.
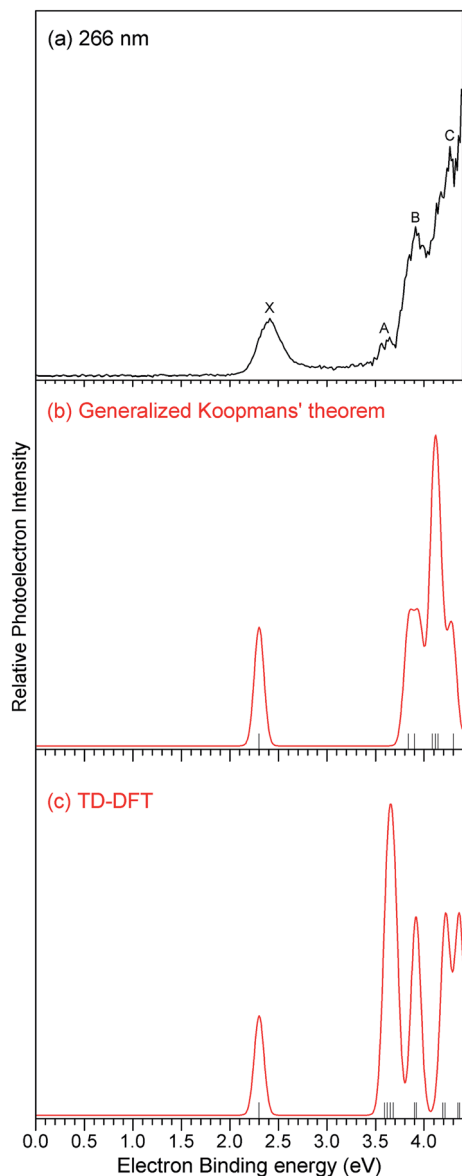
Fig. 1 (a) Photoelectron spectrum of $B_2Si_6^-$ anion recorded with 266 nm photons. (b) Simulated spectrum of $B_2Si_6^-$ anion using the generalized Koopmans' theorem. (c) Simulated spectrum of $B_2Si_6^-$ anion using the TD-DFT method. The simulations were conducted by fitting the distribution of the VDE values with unit-area Gaussian functions of 0.1 eV full width at half maximum.

Table 1 Experimental VDEs and ADE of $B_2Si_6^-$ anion measured from the 266 nm photoelectron spectrum

| | $VDE^a$ (eV) | | | | $ADE^a$ (eV) |
|---|---|---|---|---|---|
| | X | A | B | C | |
| $B_2Si_6^-$ | 2.40(8) | 3.61(8) | 3.90(8) | 4.27(8) | 2.15(8) |

[a] The numbers in parentheses indicate the uncertainties in the last digit.

# 4. Theoretical results

The structures of the typical low-lying isomers of the $B_2Si_6^-$ anion are shown in Fig. 2, and those of their corresponding neutral and cationic clusters are also shown in Fig. 2. The simulated spectra of $B_2Si_6^-$ anion using the generalized Koopmans' theorem and TD-DFT method were constructed by fitting the distribution of the VDE values with unit-area Gaussian functions of 0.10 eV full width at half maximum (Fig. 1). The relative energies, VDEs, ADEs, term energies, and NPA charges of these isomers from our calculations are summarized in Tables 2–5.

## 4.1 $B_2Si_6^-$

For the $B_2Si_6^-$ anion, the most stable isomer **1a** can be viewed as one Si atom located on the top of the distorted bowl-like $B_2Si_5$ framework. The distance between B1 and Si8 is ~2.274 Å. The Si3–Si4, Si4–Si5, Si5–Si6 and Si6–Si7 bond lengths are ~2.455 Å. The B–B bond distance is ~1.682 Å, close to the B–B bond lengths (~1.710 Å) in the compounds of the a-B (a-rhombohedral boron) type.[67] The first VDE and ADE of isomer **1a** are calculated to be 2.30 eV and 2.00 eV at the DFT/B3LYP level, respectively, in reasonable agreement with the experimental values (2.40 eV and 2.15 eV). The first term energies $\Delta E$ ($B_2Si_6(X) \leftarrow B_2Si_6(A)$) obtained from the generalized Koopmans' theorem and TD-DFT calculations are 1.59 eV and 1.36 eV, respectively, in reasonable agreement with the experimental value (1.21 eV). The second term energies $\Delta E$ ($B_2Si_6(X) \leftarrow B_2Si_6(B)$) obtained from the generalized Koopmans' theorem and TD-DFT calculations are 1.82 eV and 1.62 eV, respectively, also in reasonable agreement with the experimental measurement (1.50 eV). The second detachment channels correspond to the transitions to the two $^3A$ final states with electrons detached from HOMO−1 and HOMO−2 of $B_2Si_6^-$ anion. The third term energies $\Delta E$ ($B_2Si_6(X) \leftarrow B_2Si_6(C)$) obtained from the generalized Koopmans' theorem and TD-DFT calculations are 1.97 eV and 1.92 eV, respectively, also in good agreement with the experimental value (1.87 eV). The simulated spectra of the bowl-like isomer **1a** from the generalized Koopmans' theorem and TD-DFT calculations can reasonably explain all the observed photoelectron spectrum bands (Fig. 1). Isomer **1b** is a $C_{2h}$ distorted oblique prism with the $^2B_u$ electronic state. The theoretical VDE of isomer **1b** is calculated to be 2.98 eV, which does not match with the experimental value. Isomer **1c** is a quasi-planar structure with a boron dimer surrounded by six Si atoms. It is of $C_s$ symmetry with the $^2A'$ electronic state. The VDE and ADE of isomer **1c** are calculated to be 2.52 eV and 2.16 eV, respectively. Isomers **1b** and **1c** are less stable than isomer **1a** by 0.41 eV and 0.51 eV at the DFT/B3LYP level, respectively. The CCSD(T)/aug-cc-pVTZ results show that isomers **1b** and **1c** are higher in energy than isomer **1a** by 0.31 eV and 0.63 eV, respectively. Therefore, the existence of isomers **1b** and **1c** in the experiments can be ruled out, and isomer **1a** corresponds to the major peaks observed in the spectrum of the $B_2Si_6^-$ anion.

## 4.2 $B_2Si_6$

The lowest-energy structure of $B_2Si_6$ (isomer **2a**) with no symmetry is similar to isomer **1a** of $B_2Si_6^-$ anion. The Si3–Si4,
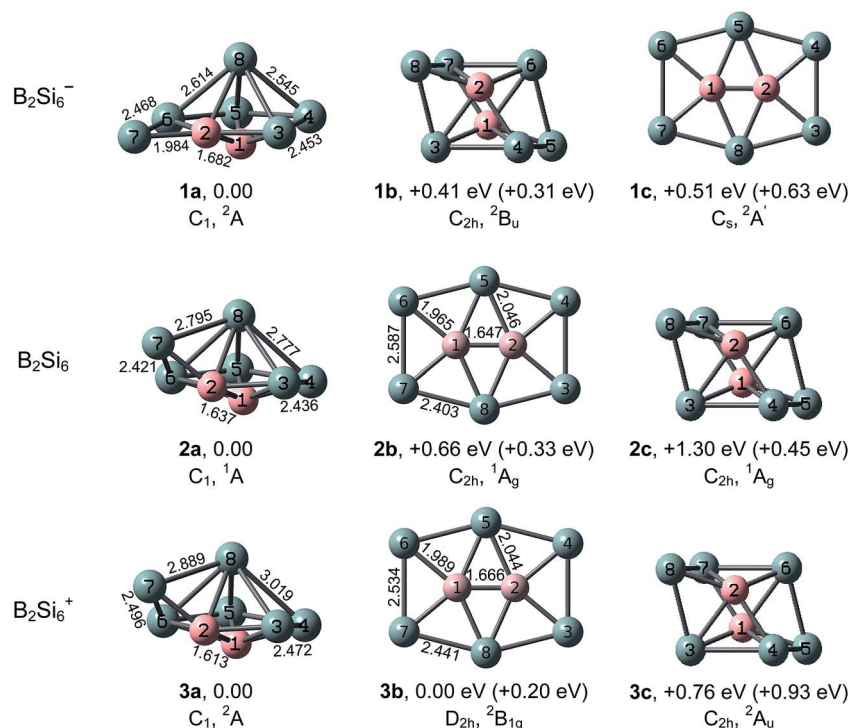
**Fig. 2** Structures and relative energies of the low-lying isomers of $B_2Si_6^q$ ($q = -1, 0, +1$). The bond distances are in angstroms. The relative energies outside the parentheses are from the DFT/B3LYP method, and those in parentheses from the CCSD(T) method.

**Table 2** Relative energies, VDEs and ADEs of the low-lying isomers of $B_2Si_6^-$ anion obtained by DFT and CCSD(T) calculations

| | | | | $\Delta E$ (eV) | | ADE (eV) | | VDE (eV) | |
|---|---|---|---|---|---|---|---|---|---|
| | Isomers | Sym. | State | B3LYP | CCSD(T) | Theo. | Expt. | Theo. | Expt. |
| $B_2Si_6^-$ | **1a** | $C_1$ | $^2A$ | 0.00 | 0.00 | 2.00 | 2.15 | 2.30 | 2.40 |
| | **1b** | $C_{2h}$ | $^2B_u$ | 0.41 | 0.31 | 2.88 | | 2.98 | |
| | **1c** | $C_s$ | $^2A'$ | 0.51 | 0.63 | 2.16 | | 2.52 | |

Si4–Si5, Si5–Si6, and Si6–Si7 bond lengths are also ~2.455 Å. The B–B bond distance is 1.637 Å, close to the B–B bond length of isomer **1a**. But the Si7–Si8 bond length is ~2.795 Å in isomer **2a**, much shorter than that (~3.820 Å) of isomer **1a**. Isomer **2b** is of $C_{2h}$ symmetry in $^1A_g$ electronic state with a boron dimer surrounded by six Si atoms. It is less stable in energy than isomer **2a** by 0.66 eV from the B3LYP/aug-cc-pVTZ calculations, while CCSD(T) calculations show that the energy difference is 0.33 eV. Isomer **2c** also has a $C_{2h}$ symmetry with the $^1A_g$ electronic state and it is higher in energy than isomer **2a** by 1.30 eV and 0.45 eV from the B3LYP and CCSD(T) calculations,

respectively. It is worth mentioning that we also considered the highly symmetric $D_{2h}$ structure of isomer **2b**, however, it is unstable.

To understand the stabilities of the isomers **2a** and **2b** of $B_2Si_6$, we searched the possible transition barriers between them by Berny method. The transition-state structure obtained by us was confirmed to connect the correct reactants (isomer **2a**)

**Table 3** Term energies of the lowest-energy isomer of $B_2Si_6^-$ anion calculated with the generalized Koopmans' theorem (GKT) and TD-DFT method

| Term energies | Expt. (eV) | GKT (eV) | TD-DFT (eV) |
|---|---|---|---|
| X ← A | 1.21 | 1.59 | 1.36 |
| X ← B | 1.50 | 1.82 | 1.62 |
| X ← C | 1.87 | 1.97 | 1.92 |

**Table 4** Relative energies, symmetries and electronic states of the low-lying isomers of $B_2Si_6$ neutral and $B_2Si_6^+$ cation obtained by the DFT/B3LYP and CCSD(T) calculations

| | | | | $\Delta E$ (eV) | |
|---|---|---|---|---|---|
| | Isomers | Sym. | State | B3LYP | CCSD(T) |
| $B_2Si_6$ | **2a** | $C_1$ | $^1A$ | 0.00 | 0.00 |
| | **2b** | $C_{2h}$ | $^1A_g$ | 0.66 | 0.33 |
| | **2c** | $C_{2h}$ | $^1A_g$ | 1.30 | 0.45 |
| $B_2Si_6^+$ | **3a** | $C_1$ | $^2A$ | 0.00 | 0.00 |
| | **3b** | $D_{2h}$ | $^2B_{1g}$ | 0.00 | 0.20 |
| | **3c** | $C_{2h}$ | $^2A_u$ | 0.76 | 0.93 |

**Table 5** NPA charges and spin density distributions of the most stable isomers (bowl-like isomers) and the quasi-planar isomers of $B_2Si_6^q$ ($q = -1, 0, +1$)

| | NPA charges | | | | | Spin density distributions | | |
|---|---|---|---|---|---|---|---|---|
| | $B_2Si_6^+$ (**3a**, $C_1$) | $B_2Si_6^+$ (**3b**, $D_{2h}$) | $B_2Si_6$ (**2a**, $C_1$) | $B_2Si_6$ (**2b**, $C_{2h}$) | $B_2Si_6^-$ (**1a**, $C_1$) | $B_2Si_6^+$ (**3a**, $C_1$) | $B_2Si_6^+$ (**3b**, $D_{2h}$) | $B_2Si_6^-$ (**1a**, $C_1$) |
| B1 | −0.62 | −0.77 | −1.04 | −0.73 | −1.02 | 0.00 | −0.05 | 0.00 |
| B2 | −0.48 | −0.77 | −1.04 | −0.73 | −1.07 | 0.15 | −0.05 | 0.08 |
| Si3 | 0.46 | 0.36 | 0.52 | 0.26 | 0.40 | 0.21 | 0.06 | 0.00 |
| Si4 | 0.34 | 0.36 | 0.37 | 0.26 | 0.07 | 0.08 | 0.06 | 0.11 |
| Si5 | 0.47 | 0.55 | 0.26 | 0.21 | 0.16 | 0.45 | 0.43 | 0.00 |
| Si6 | 0.28 | 0.36 | 0.31 | 0.26 | 0.26 | 0.04 | 0.06 | 0.00 |
| Si7 | 0.39 | 0.36 | 0.57 | 0.26 | 0.17 | 0.00 | 0.06 | 0.73 |
| Si8 | 0.16 | 0.55 | 0.05 | 0.21 | 0.03 | 0.07 | 0.43 | 0.08 |

and products (isomer **2b**) by intrinsic reaction coordinate (IRC). The transition state is determined for the conversion pathway, with a conversion barrier of 0.48 eV calculated at the CCSD(T) level. It indicates that the bowl-like structure of $B_2Si_6$ neutral (isomer **2a**) is highly stable.

### 4.3 $B_2Si_6^+$

The low-lying isomers of $B_2Si_6^+$ cation (**3a** and **3b**) are degenerated in energy from the B3LYP results. However, the CCSD(T) results show that isomer **3b** is higher than isomer **3a** by 0.20 eV in energy. The structure of isomer **3a** is similar to isomer **2a** of $B_2Si_6$. The Si7–Si8 and Si4–Si8 bond lengths are slightly elongated in isomer **3a** relative to those of isomer **2a**. Isomer **3b** has a perfectly planar hexagon structure with a large HOMO–LUMO gap of 2.35 eV. It has a $D_{2h}$ symmetry with the $^2B_{1g}$ electronic state. The Si–Si distances are somewhat different in isomer **3b**. The Si4–Si5, Si5–Si6, Si6–Si7, and Si3–Si4 bond distances are ~2.500 Å, slightly shorter than the Si7–Si8 and Si4–Si8 bonds (~2.900 Å) in the same isomer. The B–B bond length in isomer **3b** is ~1.666 Å, close to the B–B distances in the quasi-planar isomers of the negative and neutral charge states. Isomer **3c** has a $C_{2h}$ symmetry with the $^2A_u$ electronic state and it is higher in energy than isomer **3a** by 0.76 eV and 0.93 eV from the B3LYP and CCSD(T) calculations, respectively, indicating that the preference of isomer **3a** is the largest. It is worth mentioning that, for the quasi-planar or planar structures, the symmetries of the negatively charged $B_2Si_6^-$ (**1c**, $C_s$) and neutral $B_2Si_6$ (**2b**, $C_{2h}$) are lower than that of the positively charged $B_2Si_6^+$ (**3b**, $D_{2h}$), indicating that the Jahn–Teller effect caused by the increased electrons might be the major factor contributing to the lowing of the symmetry.

## 5. Discussion

### 5.1 NPA charges and spin density distributions of $B_2Si_6^q$ ($q = -1, 0, +1$)

As shown in Table 5, the effective atomic charges of the most stable structures of $B_2Si_6^q$ ($q = -1, 0, +1$) indicate that both B atoms in the clusters are negatively charged, $Q_B < 0$. It is obvious that some electrons are transferred to the B atoms, partly because of the larger Pauling electronegativity of B (2.04) as

compared to Si (1.90).[68] The electron is mainly detached from the p orbitals of Si(4) and lateral Si(7) atoms when $B_2Si_6^-$ anion with a $C_1$ symmetry was photodetached. Inversely, the electron is taken off from the B atoms when the lowest-energy isomer of $B_2Si_6$ neutral loses one electron. The spin density distributions of $B_2Si_6^-$ anion (**1a**, $C_1$) have shown that its spin densities are mainly located on lateral Si(7) and slightly located on B(2), Si(4), and Si(8). For $B_2Si_6^+$ cation (**3a**, $C_1$), the spin densities are mainly located on B(2), Si(3), and Si(5). For planar $B_2Si_6^+$ cation (**3b**, $D_{2h}$), the unpaired electron is mainly located on the $C_2$ axis of Si(5) and Si(8).

### 5.2 Molecular orbitals of $B_2Si_6$ (**2a**, $C_1$)

Using the 'adaptive density partitioning' approach,[65] one can also approximately extract 9 delocalized valence MOs of approximate "s" and "p" symmetry for the remaining 30 electrons in the $B_2(2s^22p^1)$–$Si_6(3s^23p^2)$ valence shell of $B_2Si_6$ (**2a**, $C_1$) (Fig. 3), in addition to the 6 lone pair electrons of six Si atoms, 9 delocalized MOs include one 2c-2e BSi σ bond (electronic occupation is equal to 1.88 |e|), three 3c-2e $B_2Si$ or $BSi_2$ σ bonds
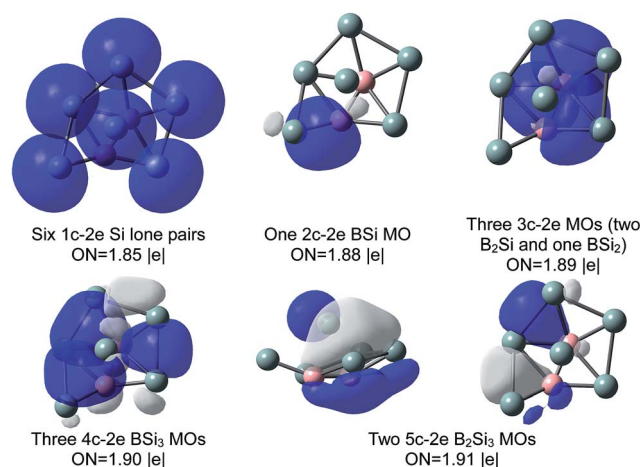


Six 1c-2e Si lone pairs
ON=1.85 |e|

One 2c-2e BSi MO
ON=1.88 |e|

Three 3c-2e MOs (two $B_2Si$ and one $BSi_2$)
ON=1.89 |e|

Three 4c-2e $BSi_3$ MOs
ON=1.90 |e|

Two 5c-2e $B_2Si_3$ MOs
ON=1.91 |e|

**Fig. 3** Molecular orbitals of the bowl-like isomer of $B_2Si_6$ (**2a**, $C_1$). Six lone pairs of Si atoms and nine optimally localized MOs (contour values $\psi = \pm 0.038$ au) are from the AdNDP[65] method (ON = electronic occupation).

(electronic occupation is equal to 1.89 |e|), three 4c-2e $BSi_3$ σ bonds (electronic occupation is equal to 1.90 |e|), and two 5c-2e $B_2Si_3$ MOs (electronic occupation is equal to 1.91 |e|). The 15 electron pairs of these 30e systems cannot be localized symmetrically. The two 5c-2e $B_2Si_3$ MOs contain the σ plus π double delocalization. The Si7–Si8 bond length in isomer **2a** is shortened by 1.025 Å relative to that of isomer **1a**, most likely due to the forming of the 4c-2e $BSi_3$ σ bonds.

# 6.   Conclusions

We measured the photoelectron spectrum of $B_2Si_6^-$ anion and investigated its anionic, cationic and neutral structures with density functional theory (B3LYP) and wave function theory (CCSD(T)) approaches. By comparing the calculated VDEs with the experimental measurements, the structure of $B_2Si_6^-$ anion is determined. The CCSD(T) results reveal that the lowest-lying isomers of $B_2Si_6^q$ ($q = -1, 0, +1$) have a peculiar structure with a Si atom hanging over a distorted bowl-like $B_2Si_5$ framework. The Si7–Si8 distance in the lowest-lying isomer **2a** of $B_2Si_6$ neutral is shortened by 1.025 Å relative to that of the lowest-lying isomer **1a** of $B_2Si_6^-$ anion. Isomer **2a** is characterized with σ or π delocalization in chemical bonding. In addition to the bowl-like structures, we also found low-lying quasi-planar or planar structures for $B_2Si_6^q$ ($q = -1, 0, +1$), which are higher in energy than the corresponding bowl-like structures by at least 0.20 eV. The planar $B_2Si_6^+$ cation has a $D_{2h}$ symmetry and is highly aromatic. For the quasi-planar or planar structures, the symmetries of the negatively charged $B_2Si_6^-$ (**1c**, $C_s$) and neutral $B_2Si_6$ (**2b**, $C_{2h}$) are lower than that of the positively charged $B_2Si_6^+$ (**3b**, $D_{2h}$), more likely due to the Jahn–Teller effect upon the addition of electrons.

# Notes and references

1 H. Hiura, T. Miyazaki and T. Kanayama, *Phys. Rev. Lett.*, 2001, **86**, 1733–1736.
2 S. N. Khanna, B. K. Rao and P. Jena, *Phys. Rev. Lett.*, 2002, **89**, 016803.
3 A. Fleurence, R. Friedlein, T. Ozaki, H. Kawai, Y. Wang and Y. Yamada-Takamura, *Phys. Rev. Lett.*, 2012, **108**, 245501.
4 L. Chen, C.-C. Liu, B. Feng, X. He, P. Cheng, Z. Ding, S. Meng, Y. Yao and K. Wu, *Phys. Rev. Lett.*, 2012, **109**, 056804.
5 V. Kumar and Y. Kawazoe, *Phys. Rev. Lett.*, 2003, **90**, 055502.
6 Y. Cui, X. Duan, J. Hu and C. M. Lieber, *J. Phys. Chem. B*, 2000, **104**, 5213–5216.
7 G. Cantele, E. Degoli, E. Luppi, R. Magri, D. Ninno, G. Iadonisi and S. Ossicini, *Phys. Rev. B: Condens. Matter Mater. Phys.*, 2005, **72**, 113303.
8 C. F. Cline, *Nature*, 1958, **181**, 476–477.
9 C. F. Cline and D. E. Sands, *Nature*, 1960, **185**, 456.
10 R. West, M. J. Fink and J. Michl, *Science*, 1981, **214**, 1343–1344.
11 S. Ishida, T. Iwamoto, C. Kabuto and M. Kira, *Nature*, 2003, **421**, 725–727.
12 A. Sekiguchi and V. Y. Lee, *Chem. Rev.*, 2003, **103**, 1429–1448.
13 M. Weidenbruch, *Angew. Chem., Int. Ed.*, 2003, **42**, 2222–2224.
14 N. Tokitoh, *Acc. Chem. Res.*, 2004, **37**, 86–94.
15 A. G. Brook, F. Abdesaken, B. Gutekunst, G. Gutekunst and R. K. Kallury, *J. Chem. Soc., Chem. Commun.*, 1981, 191–192.
16 A. Sekiguchi, R. Kinjo and M. Ichinohe, *Science*, 2004, **305**, 1755–1757.
17 Y. Wang, Y. Xie, P. Wei, R. B. King, H. F. Schaefer, P. v. R. Schleyer and G. H. Robinson, *Science*, 2008, **321**, 1069–1071.
18 H. Ottosson and P. G. Steel, *Chem.–Eur. J.*, 2006, **12**, 1576–1585.
19 M. Weidenbruch, *Angew. Chem., Int. Ed.*, 2006, **45**, 4241–4242.
20 M. Kira and T. Iwamoto, *Adv. Organomet. Chem.*, 2006, **54**, 73–148.
21 T. Sasamori, J. S. Han, K. Hironaka, N. Takagi, S. Nagase and N. Tokitoh, *Pure Appl. Chem.*, 2010, **82**, 603–612.
22 K. Abersfelder, A. J. White, H. S. Rzepa and D. Scheschkewitz, *Science*, 2010, **327**, 564–566.
23 T. Agou, Y. Sugiyama, T. Sasamori, H. Sakai, Y. Furukawa, N. Takagi, J.-D. Guo, S. Nagase, D. Hashizume and N. Tokitoh, *J. Am. Chem. Soc.*, 2012, **134**, 4120–4123.
24 T. Sasamori, K. Hironaka, Y. Sugiyama, N. Takagi, S. Nagase, Y. Hosoi, Y. Furukawa and N. Tokitoh, *J. Am. Chem. Soc.*, 2008, **130**, 13856–13857.
25 M. Ichinohe, M. Igarashi, K. Sanuki and A. Sekiguchi, *J. Am. Chem. Soc.*, 2005, **127**, 9978–9979.
26 V. Y. Lee, K. Takanashi, T. Matsuno, M. Ichinohe and A. Sekiguchi, *J. Am. Chem. Soc.*, 2004, **126**, 4758–4759.
27 A. D. Zdetsis, *J. Chem. Phys.*, 2007, **127**, 214306.
28 D. Jose and A. Datta, *J. Phys. Chem. C*, 2012, **116**, 24639–24648.
29 S. Nagase, H. Teramae and T. Kudo, *J. Chem. Phys.*, 1987, **86**, 4513–4517.
30 K. K. Baldridge, O. Uzan and J. M. Martin, *Organometallics*, 2000, **19**, 1477–1487.
31 C. Gerdes and T. Müller, *Angew. Chem., Int. Ed.*, 2010, **49**, 4860–4862.
32 K. Abersfelder, A. J. White, R. J. Berger, H. S. Rzepa and D. Scheschkewitz, *Angew. Chem., Int. Ed.*, 2011, **123**, 8082–8086.
33 K. Abersfelder, A. J. White, R. J. Berger, H. S. Rzepa and D. Scheschkewitz, *Angew. Chem., Int. Ed.*, 2011, **50**, 7936–7939.
34 D. Kratzert, D. Leusser, J. J. Holstein, B. Dittrich, K. Abersfelder, D. Scheschkewitz and D. Stalke, *Angew. Chem., Int. Ed.*, 2013, **52**, 4478–4482.
35 A. S. Ivanov and A. I. Boldyrev, *J. Phys. Chem. A*, 2012, **116**, 9591–9598.
36 M. Takahashi and Y. Kawazoe, *Organometallics*, 2005, **24**, 2433–2440.

37 M. Takahashi and Y. Kawazoe, *Chem. Phys. Lett.*, 2006, **418**, 475–480.

38 M. Takahashi and Y. Kawazoe, *Comput. Mater. Sci.*, 2006, **36**, 30–35.

39 X. Tan, F. Li and Z. Chen, *J. Phys. Chem. C*, 2014, **118**, 25825–25835.

40 D. N. Bernardo and G. H. Morrison, *Surf. Sci.*, 1989, **223**, L913–L919.

41 A. I. Boldyrev and J. Simons, *J. Phys. Chem.*, 1993, **97**, 1526–1532.

42 J. L. B. Knight, A. J. McKinley, R. M. Babb, M. D. Morse and C. A. Arrington, *J. Chem. Phys.*, 1993, **98**, 6749–6757.

43 G. Verhaegen, F. E. Stafford and J. Drowart, *J. Chem. Phys.*, 1964, **40**, 1622–1628.

44 R. Viswanathan, R. W. Schmude and K. A. Gingerich, *J. Phys. Chem.*, 1996, **100**, 10784–10786.

45 J. Yamauchi, N. Aoki and I. Mizushima, *Phys. Rev. B: Condens. Matter Mater. Phys.*, 1997, **55**, R10245.

46 R. Davy, E. Skoumbourdis and D. Dinsmore, *Mol. Phys.*, 2005, **103**, 611–619.

47 Z. Sun, Z. Yang, Z. Gao and Z. Tang, *Rapid Commun. Mass Spectrom.*, 2007, **21**, 792–798.

48 E. Bourgeois and X. Blase, *Appl. Phys. Lett.*, 2007, **90**, 142511.

49 X. Pi, X. Chen and D. Yang, *J. Phys. Chem. C*, 2011, **115**, 9838–9843.

50 N. M. Tam, T. B. Tai and M. T. Nguyen, *J. Phys. Chem. C*, 2012, **116**, 20086–20098.

51 J. Dai, Y. Zhao, X. J. Wu, J. L. Yang and X. C. Zeng, *J. Phys. Chem. Lett.*, 2013, **4**, 561–567.

52 N. X. Truong, M. Haertelt, B. K. Jaeger, S. Gewinner, W. Schöllkopf, A. Fielicke and O. Dopfer, *Int. J. Mass Spectrom.*, 2016, **395**, 1–6.

53 H.-G. Xu, Z.-G. Zhang, Y. Feng, J. Yuan, Y.-C. Zhao and W.-J. Zheng, *Chem. Phys. Lett.*, 2010, **487**, 204–208.

54 M. J. Frisch, *et al.*, *Gaussian 09 Revision D.01*, Gaussian Inc., Wallingford CT, 2009.

55 H.-J. Zhai, Y.-F. Zhao, W.-L. Li, Q. Chen, H. Bai, H.-S. Hu, Z. A. Piazza, W.-J. Tian, H.-G. Lu and Y.-B. Wu, *Nat. Chem.*, 2014, **6**, 727–731.

56 H. J. Werner, P. J. Knowles, G. Knizia, F. R. Manby and M. Schütz, *et al.*, *MOLPRO, Version 2012.1*, A Package of ab Initio Programs, see http://www.molpro.net.

57 B. Sengupta, C. M. Ritchie, J. G. Buckman, K. R. Johnsen, P. M. Goodwin and J. T. Petty, *J. Phys. Chem. C*, 2008, **112**, 18776–18782.

58 K. Gillen, R. Jensen and N. Davidson, *J. Am. Chem. Soc.*, 1964, **86**, 2792–2796.

59 M. Seth and T. Ziegler, *J. Chem. Theory Comput.*, 2012, **8**, 901–907.

60 C. F. Guerra, J. Snijders, G. Te Velde and E. Baerends, *Theor. Chem. Acc.*, 1998, **99**, 391–403.

61 G. Te Velde, F. M. Bickelhaupt, E. J. Baerends, C. Fonseca Guerra, S. J. van Gisbergen, J. G. Snijders and T. Ziegler, *J. Comput. Chem.*, 2001, **22**, 931–967.

62 See http://www.scm.com for ADF2012.01 and ADF2013.01, SCM, Theoretical Chemistry, Vrije Universiteit, Amsterdam, The Netherlands.

63 A. E. Reed, L. A. Curtiss and F. Weinhold, *Chem. Rev.*, 1988, **88**, 899–926.

64 A. E. Reed and F. Weinhold, *J. Chem. Phys.*, 1983, **78**, 4066.

65 D. Y. Zubarev and A. I. Boldyrev, *Phys. Chem. Chem. Phys.*, 2008, **10**, 5207–5217.

66 T. Lu and F. Chen, *J. Comput. Chem.*, 2012, **33**, 580–592.

67 B. Albert and H. Hillebrecht, *Angew. Chem., Int. Ed.*, 2009, **48**, 8640–8668.

68 L. C. Allen, *J. Am. Chem. Soc.*, 1989, **111**, 9003–9014.